Science of the Total Environment 914 (2024) 169925

Contents lists available at ScienceDirect

Science of the Total Environment

journal homepage: www.elsevier.com/locate/scitotenv

Pluvial flood risk assessment for 2021–2050 under climate change scenarios in the Metropolitan City of Venice

Elena Allegri [a,b], Marco Zanetti [a], Silvia Torresan [a,b], Andrea Critto [a,b,*]

[a] Department of Environmental Sciences, Informatics and Statistics, University Ca' Foscari Venice, via Torino 155, 30175 Venezia, Italy
[b] Centro Euro-Mediterraneo sui Cambiamenti Climatici (CMCC), via Marco Biagio 5, 73100 Lecce, Italy

HIGHLIGHTS

- Future pluvial flood scenarios performed with ML methodology are proposed.
- Forward features selection and spatio-temporal CV permit to predict pluvial flood occurrence.
- LR model was the most accurate model to predict pluvial flood events.
- Risk maps of pluvial flood are developed for future scenarios of climate change (RCPs 4.5 and 8.5).
- Managing pluvial flood risk can increase climate resilience in the MCV.

GRAPHICAL ABSTRACT

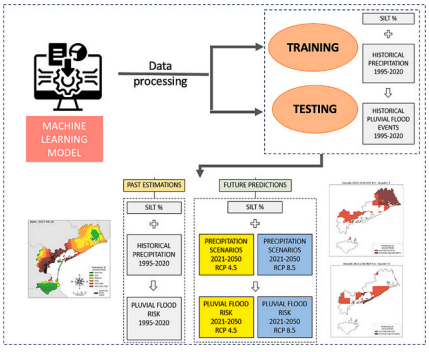

ARTICLE INFO

Editor: Damia Barcelo

Keywords:
Cumulative rainfall
Machine learning
Spatio-temporal cross-validation
Extreme events
Future scenarios

ABSTRACT

Pluvial flood is a natural hazard occurring from extreme rainfall events that affect millions of people around the world, causing damages to their properties and lives. The magnitude of projected climate risks indicates the urgency of putting in place actions to increase climate resilience. Through this study, we develop a Machine Learning (ML) model to predict pluvial flood risk under Representative Concentration Pathways (RCP) 4.5 and 8.5 for future scenarios of precipitation for the period 2021–2050, considering different triggering factors and precipitation patterns. The analysis is focused on the case study area of the Metropolitan City of Venice (MCV) and considers 212 historical pluvial flood events occurred in the timeframe 1995–2020. The methodology developed implements spatio-temporal constraints in the ML model to improve pluvial flood risk prediction under future scenarios of climate change. Accordingly, a cross-validation approach was applied to frame a model able to predict pluvial flood at any time and space. This was complemented with historical pluvial flood data and the selection of nine triggering factors representative of territorial features that contribute to pluvial flood events. Logistic Regression was the most reliable model, with the highest AUC score, providing robust result both in the validation and test set. Maximum cumulative rainfall of 14 days was the most important feature contributing to pluvial flood occurrence. The final output is represented by a suite of risk maps of the flood-prone areas in the MCV for each quarter of the year for the period 1995–2020 based on historical data, and risk maps for each quarter of the period 2021–2050 under RCP4.5 and 8.5 of future precipitation scenarios. Overall, the results

* Corresponding author.
E-mail address: critto@unive.it (A. Critto).

https://doi.org/10.1016/j.scitotenv.2024.169925
Received 31 July 2023; Received in revised form 18 December 2023; Accepted 3 January 2024
Available online 8 January 2024

underline a consistent increase in extreme events (i.e., very high and extremely high risk of pluvial flooding) under the more catastrophic scenario RCP8.5 for future decades compared to the baseline.

1. Introduction

Despite the risk reduction efforts and billions invested in flood protection actions put in place by governmental institutions, floods continue to be a serious issue causing several damages and injuring people (Kundzewicz et al., 2013). Moreover, it is expected that changes in precipitation patterns (e.g. extreme rainfall) prompted by climate change will increase the intensity and frequency of weather-related disasters including flash floods, riverine and coastal flooding, and pluvial floods in many regions (Asadieh and Krakauer, 2017) (IPCC, 2021). The IPCC predicts that climate-related extreme events will become more frequent, will affect multiple sectors and will cause systematic failures across Europe, leading to greater economic losses. Particularly, climate change is already affecting the occurrence, intensity, and spatial distribution of extreme weather events. Among these, pluvial flooding, that occurs when water runoff exceeds infiltration rates and drainage capacity (frequently during short-duration and high-intensity rainfall events) (Wheater, 2006; Miller and Hutchins, 2017), results from the combination of unfavorable hydrological, meteorological and geomorphological conditions, as well as a failure of flood protection structures or improper early warning systems (Roy et al., 2020). Furthermore, to the undeniable effects of global warming, anthropogenic factors, primarily urban sprawl and population growth, have increased the magnitude of flood runoffs and have amplified the flood damage potential (Kundzewicz et al., 2013; UNISDR, 2015; Szewrański et al., 2018). They constitute an increasing vulnerability of the territories, which have a reduced capability to absorb surface runoff and are more exposed to damages, both economic and to people and assets (Blanc et al., 2012; Miller and Hutchins, 2017). The extent of economic losses and the number of individuals displaced by flooding events has already increased globally (Roy et al., 2020). According to the United Nations World Water Development Report (UNESCO, 2020), in the last decades Europe has counted >6 million people affected by flood events and economic damages for more than US$86 billion. In this context, flood risk management has become even more significant, pushing many governments and decision makers to recognize the need of developing resilient flood management strategies and policies for sustainable urban development (Herath and Wijesekera, 2019), as highlighted also by the Sendai Framework for Disaster Risk Reduction (UNISDR, 2015). Accordingly, this paper aims at increasing the current knowledge and awareness on the risks of pluvial flood arising in urban areas due to future scenarios of climate change.

Despite over the last years the interest in pluvial flood risk is grown steadily as response to flood events occurred in Europe, few methodologies have been developed for studying pluvial flood events under climate scenarios (Sperotto et al., 2015; Szewrański et al., 2018; Peleg et al., 2022; Jiang et al., 2023; Ebers et al., 2023). The methodological approaches developed so far concern Storm Water Management Model for assessing the impacts of urbanization on runoff and flood reduction while applying low impact development actions (Ahiablame and Shakya, 2016); Hydrodynamic Model of Urban Drainage System (Nowakowska et al., 2017), Regional Risk Assessment (Sperotto et al., 2015), and combined fluvial-pluvial hazard assessment based on the probability of flood occurrence (Apel et al., 2016). However, these approaches do not include climate change scenarios and gaps exist in knowledge and research concerning pluvial flood modelling, risk assessment and management (Apel et al., 2016; Szewrański et al., 2018). The majority of modelling techniques developed for studying pluvial flood risk in urban areas uses hydraulic and hydrodynamic models, Geographic Information System (GIS) and Remote Sensing (RS) techniques, and Multi-Criteria Decision Analysis (MCDA) functions (Zanetti et al., 2022). However, these methodologies present some intrinsic limitations (e.g., require complex input data, high computational time and costs, high dependence on expert knowledge, strong decision-makers assumptions) (Chowdary et al., 2013; Khosravi et al., 2019; Wagenaar et al., 2020; Guo et al., 2021), which fostered the scientific community to explore and test new methodologies able to overcome these challenges, such as through Machine Learning (ML) models (Zennaro et al., 2021). Over the last years, the use of ML methods to predict natural hazard risks has massively increased, due to their high performance and predictive capability (Ahmadlou et al., 2019; Zanetti et al., 2022). Particularly, the most widespread ML techniques have focused on incorporating GIS-based flood models and RS tools for the spatial analysis of large volume of data on natural hazards. The majority of methods used so far include Artificial Neural Networks (Kia et al., 2012; Aslan et al., 2022), Frequency Ratio (Lee et al., 2012; Rahmati et al., 2016), Logistic Regression (Pradhan, 2009; Pham et al., 2020), Decision Trees (Tingsanchali and Karim, 2010; Merz et al., 2013; Tehrany et al., 2013), Support Vector Machines (Deng et al., 2013; Tehrany et al., 2014), Random Forest (Roy et al., 2020), Evidence Belief Function (Chowdhuri et al., 2020). These models are useful to identify flood-prone areas, but do not consider spatio-temporal constraints and they have not been tested under climate change scenarios.

Drawing on such considerations, the aim of the analysis presented here is to develop a ML model able to foresee robust scenarios of pluvial flood in the medium-long term. The method is based on historical pluvial flood data to predict the pluvial flood risk in the Metropolitan City of Venice (Northern Italy) for each quarter of the period 1995–2020. Then, the developed ML model is used to predict pluvial flood risk under the Representative Concentration Pathways (RCP) 4.5 and 8.5 scenarios of future precipitation for the time period 2021–2050. The ML model builds on the relationship between a set of input variables, called features, and an output variable, called response variable. In this work, the response variable is represented by the occurrence or not of a pluvial flood for each specific area of the MCV, while the features are represented by precipitation and triggering factors that characterize the territory. These features might positively or negatively affect the flooding occurrence in a specific area and time. Therefore, the collected data (e.g., triggering factors, precipitation and historical pluvial flood data) constitute the dataset used to build up the model.

The presented ML methodology builds up on the ML model developed in Zanetti et al. (2022) on the baseline scenario of pluvial flood risk for the Metropolitan City of Venice for the period 1995–2020.

2. Case study area: the metropolitan city of Venice

The study area for the pluvial flood risk assessment under future climate change scenarios is represented by the administrative boundaries of the Metropolitan City of Venice (MCV), located in the Veneto region, in the North East coast of the Adriatic Sea (Fig. 1). It consists of 44 municipalities and has an extension of 2467 km^2 for an overall population of 839.396 inhabitants (ISTAT, 2022), mainly concentrated around the two biggest urban centers of Mestre and Venice. The territory includes both the small island around the Venice lagoon and the mainland, in which resides most of the population. In the area, multiple and diversified economic activities have taken place, ranging from industries (e.g., the petrochemical industry of Marghera district), shipping, seaport activities, to tourism and fishing activities along the coast (Dipartimento per gli Affari Regionali e le Autonomie, 2017). The urbanization development of the CMV is primarily due to the economic growth after the World War II and the expansion of the petrochemical plant of Porto Marghera, which led to a rapid urbanization sprawl of the area. This

development led to a growing demand of residential areas and infrastructures, at the expense of green areas that were converted into urban zones. These changes determined structural hydraulic criticalities that were partially overcome with new public green areas (Venice Province, 2011). Despite the implementation of such measures, many criticalities remain due to improper sewer and drainage systems, especially during severe rainfall events. These criticalities might become an obstacle with the future climate scenarios, according to which will increase the frequency and intensity of extreme rainfall events in the Mediterranean region (Spano et al., 2020; IPCC, 2021). Specifically, in Northern Italy is expected a precipitation reduction during the summer period and an increase in precipitation for the winter period (Spano et al., 2020). Beside the climate drivers, the geological, hydrological and social (e.g., growing population rate in urban areas) and structural (e.g., urbanization rate, sewage system) factors will directly contribute to increase the vulnerability of the territory and limit the soil absorption capability, exposing local communities to pluvial flood events (Spano et al., 2020). These criticalities already showed up during a flooding event occurred in September 2007 in the city center of Mestre, with 260.4 mm of precipitation in 24 h (ARPAV, 2007). However, similar events occurred from 2000 to 2009 in the same areas, causing extensive economic damages to goods and people (Venice Province, 2011). As a result, a comprehensive study able to incorporate climate change scenarios in predicting pluvial flood risk is essential to aid decision- and policy makers in defining adaptation measures in the medium and long term. For this aim, and to develop a robust model able to predict pluvial flood events, territorial features (e.g., land use, aspect, curvature, permeability, slope, etc.) have been included, as detailed in Chapter 3.1.

3. Material and methods

To assess pluvial flood risk, territorial features and precipitation data, varying both in time and space, have been analyzed, and for which a specific methodology considering spatio-temporal constraints needs to be developed. The flowchart in Fig. 2 outlines the main steps of the ML methodology implemented to identify pluvial flood risk areas under future scenarios of climate change.

In the first step triggering factors and historical pluvial flood data have been collected to create the dataset used to fit the ML model (Sections 3.1 and 3.2). The input data have been divided in multiple data sets, used in different stages of the creation of the ML model: training and test set (Sections 3.3 and 3.4). Then, cross validation approaches were used to further split the training set into training and validation set (Section 3.5). In this case study, the validation set was used for hyperparameters tuning as well as to select the main features to consider for improving the prediction of pluvial flood areas. The hyperparameters tuning was applied to define the structure of the model and to control the learning process of the model itself. Four ML models were tested and their accuracy was evaluated. Finally, the best model was selected to predict pluvial flood events considering future scenarios of climate change, under RCP4.5 and 8.5 (Section 3.6).

3.1. Data collection and preprocessing

3.1.1. Triggering factors

Pluvial flood can or cannot occur in an area according to the morphology of the territory. In predicting pluvial flood events, a set of triggering factors, used as learning variables by the model, were identified to predict the response variable (i.e., flooded areas) at a different time and location. They represent territory's features that might positively or negatively affect the occurrence of flooding events. In this study, 9 triggering factors have been selected, identified according to the literature (e.g., Arabameri et al., 2019; Wang et al., 2020; Shahabi et al., 2021) and, particularly, the available data, from which part of the triggering factors were derived (e.g., distance to road, distance to river). The dataset and maps available restricted the characterization of the MCV to 9 territorial features, considered also the most relevant in shaping the risk of pluvial flood in the study area (Fig. A in SM). Specifically, the features considered are: aspect, curvature, distance to river, distance to road, land use, Normalized Difference Vegetation Index (NDVI), permeability, slope and texture. These triggering factors include information about the characteristics of the case study area of the MCV, and, only for the land use, the time in which the territory has these characteristics. The triggering factors can be classified as numerical, when their values are numbers, or as categorical, when they are grouped in classes. Aspect is the direction or orientation of the maximum slope of the surface and it has been considered in four categories according to different angle ranges: North (45°-135°), West (135°-225°), South (225°-315°), and East (315°-45°). Curvature is the degree of distortion of the slope surface and it has been differentiated into three classes: flat, concave or convex. Distance to road indicates the proximity to artificial infrastructure and it has been considered both as numerical and as categorical in three classes (0 m - 250 m, 250 m - 500 m, >500 m). Distance to river indicates the proximity to river networks and it has been considered both as numerical and as categorical in three classes (0 m - 250 m, 250 m - 500 m, >500 m). Land use is the specific land types and have been considered four main classes of land use: agricultural areas, green areas, industrial areas and urban areas. Land use data were collected for five different years: 1990, 2000, 2006, 2012, and 2018. Normalized Difference Vegetation Index (NDVI) indicates the vegetation density extracted from satellite images; it has been considered as numerical. Permeability is an indicator of water infiltration and it is

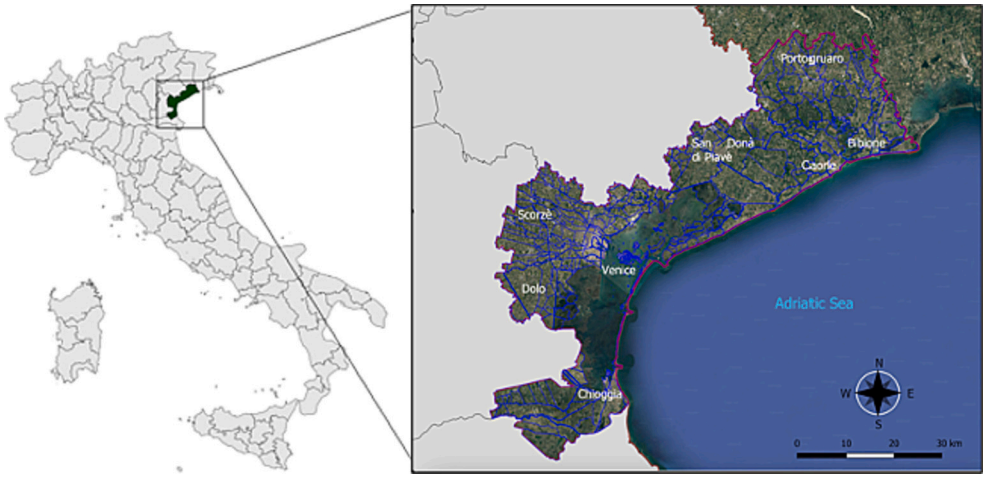

Fig. 1. The case study area: the Metropolitan City of Venice with the water basins flowing in.

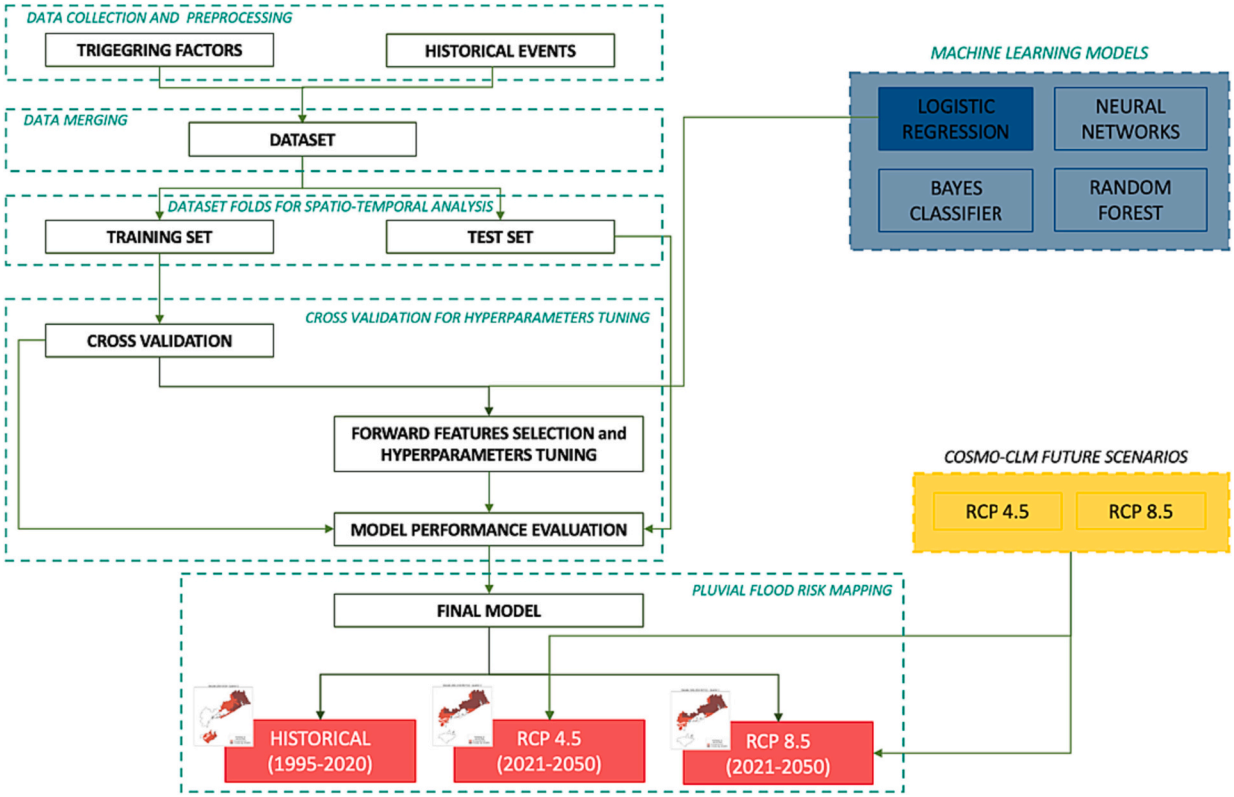

Fig. 2. Flowchart of the ML methodology to predict pluvial flood risk under future climate scenarios.

numerically expressed in millimeters per hour (mm/h). Slope is the inclination of the surface and it has been considered in two classes: presence or absence of slope. Texture is a soil infiltration property, classified by the percentage composition of its solid particles distinguished in granulometric characteristics as the percentage of sand, silt, clay, quartz and porosity. Table 1 lists the triggering factors and their data sources.

3.1.2. Historical pluvial flood data

A dataset of historical pluvial flood events recorded between 1995 and 2020 was provided by the Metropolitan City of Venice (https://webgis2.cittametropolitana.ve.it) with detailed information regarding the localization and extent of flooded areas for each event. 212 daily events were grouped by dividing the year in four periods of three months each and combining them to get more reliable information on the flooded areas occurred in a specific time period with respect to a daily event. Fig. 3 shows the percentage of case study areas that were inundated at least once in each quarter of the time period 1995–2020. From the figure, it can be noticed that the periods with major flooding events occurred in the 3rd quarter (i.e., months from July to September) of 2007 (4.24 %), 1st quarter (i.e., months from January to March) of 2013 (2.92 %) and 1st quarter of 2014 (4.06 %). Notice that, in the period between 1996 and 2005, only two pluvial flood events were recorded.

3.1.3. Historical precipitation

Precipitation is expected to be the main indicator related to pluvial flood occurrence. Historical precipitation data were provided by the Regional Agency for Environmental Prevention and Protection of Veneto (ARPAV) for each day of the period between January 1995 and October 2020. Precipitation features were extracted for each quarter based on the maximum cumulative precipitation in 1 day, 2 to 14 consecutive days, 21 consecutive days, 28 consecutive days and 90 consecutive days. Also, indicators of the number of times that daily cumulative precipitation reached 10 mm, 20 mm, 30 mm, 40 mm and 50 mm in three months were collected. Overall, 17 features were extracted for cumulative precipitation and 5 features to count the reaching of specific levels of rainfall (10 to 50 mm). Since the meteorological stations do not cover all the study area, the spatial distribution of precipitation was computed by interpolating the 188 stations placed across Veneto region using the Inverse Distance Weighting (IDW) method. It is noticeable that ML models' performance can vary according to the quality of the input data, hence precipitation was

Table 1
The triggering factors collected and their data sources. Digital Terrain Model (DTM) and Agenzia Regionale per la Prevenzione e Protezione Ambientale del Veneto (ARPAV).

Triggering factors	Spatial resolution	Temporal resolution	Features	Variable type	Data source
Aspect	25 m	2019	4	Categorical	DTM Veneto Region
Curvature	25 m	2019	3	Categorical	DTM Veneto Region
Distance to river	–	2020	4	Categorical / Numerical	Metropolitan City of Venice
Distance to road	–	2019	4	Categorical / Numerical	Metropolitan City of Venice
Land use	100 m	1990–2018	4	Categorical	CORINE Land Cover
Normalized Difference Vegetation Index (NDVI)	10 m	2015	1	Numerical	Sentinel 2 - Earth Explorer
Permeability	–	2016	1	Numerical	ARPAV
Slope	25 m	2019	1	Categorical	DTM Veneto Region
Texture	–	2016	5	Numerical	ARPAV

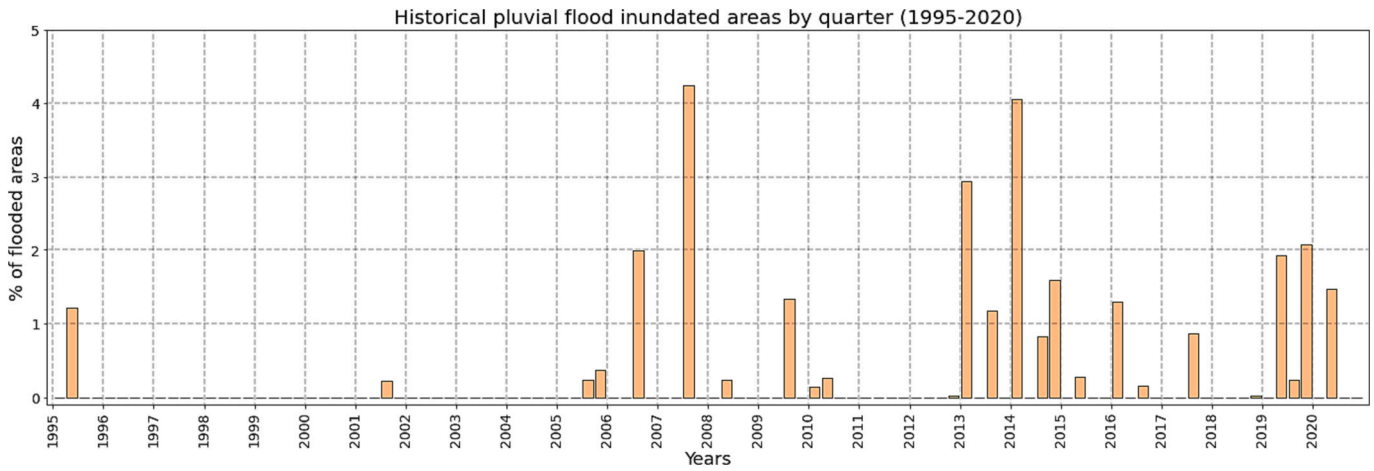

Fig. 3. The percentage of reported flooded areas in the time period 1995–2020 in the Metropolitan City of Venice.

interpolated considering different combinations of meteorological stations: 3, 5, 7 or 9 closest stations. Fig. 4 shows the 95th percentile of the cumulative precipitation in 1 and 14 days for each quarter of the period of analysis, identifying the worst day and 14 cumulative days of rainfall in the quarter. Each bar displays that there has been at least 5 days (for 1 day of rain) or 5 periods of 14 days of cumulative rainfall in which the value was above the value reported on the y-axis. From the figure we can see that the most intense daily cumulative precipitation was recorded in the 3rd quarter of 2007 (153 mm of rainfall) while the most intense 14 consecutive days of cumulative precipitation were recorded in the 1st quarter of 2014 (352 mm of rainfall). Overall, highest is the bar in the chart, more extreme rainfall events have occurred in the quarter. Therefore, according to Fig. 4, most extreme events occur mainly in autumn (4th quarter) with peaks in winter and spring, while the summer period experiences reduced precipitations. However, an overall constant increasing trend of extreme events can be identified for the historical period.

3.1.4. *Future precipitation scenarios*

In Section 3.1.3 historical precipitation from meteorological stations were introduced to relate rainfall to pluvial flood events of the past. In this section, future precipitation collected from a different data source are presented to get a future estimation of rainfall events. Since future pluvial flood events were not yet occurred, only historical precipitation was used to study the effect of rainfall on pluvial flood.

Future precipitation data were collected from the regional COSMO Climate Change (COSMO-CLM) model that simulates daily cumulative precipitation under the Representative Concentration Pathways (RCP) 4.5 and 8.5. The COSMO-CLM model reports the predictions for the time period 2006–2100 covering the MCV with a spatial resolution of 8 km. Fig. 5 (a) shows the 95th percentile of the cumulative precipitation for 1 and 14 consecutive days for each quarter of each year for the time period 2021–2050 under RCP 4.5. From the figure we can see that the most intense precipitation day would be predicted for the 4th quarter of 2044 (130 mm of rainfall), while the most intense 14 consecutive days would be expected for the 4th quarter of 2026 (256 mm of rainfall). Under RCP4.5 scenario, the extreme events under 14 days of cumulative precipitation do not exceed the 250 mm of rainfall, which are instead overcome multiple times under RCP8.5. Fig. 5 (b) shows the 95th percentile of the cumulative precipitation for 1 and 14 days under RCP 8.5 and can be noticed that the most intense precipitation day and the most intense 14 consecutive days would be in the 3rd quarter of 2047 (182 and 343 mm, respectively). In general, highest is the bar more extreme events are expected in the future under the two RCPs scenarios and, specifically, RCP 8.5 scenario is expected to have more extreme precipitation events compared to RCP 4.5 scenario. The results show higher values of cumulative precipitation in the 1st and 4th quarters and an overall constant increasing trend, with more extreme rainfall events alternated to limited precipitations under RCP8.5.

3.2. *Data merging*

Once collected and preprocessed the triggering factors, historical pluvial flood data and precipitation data, they need to be merged

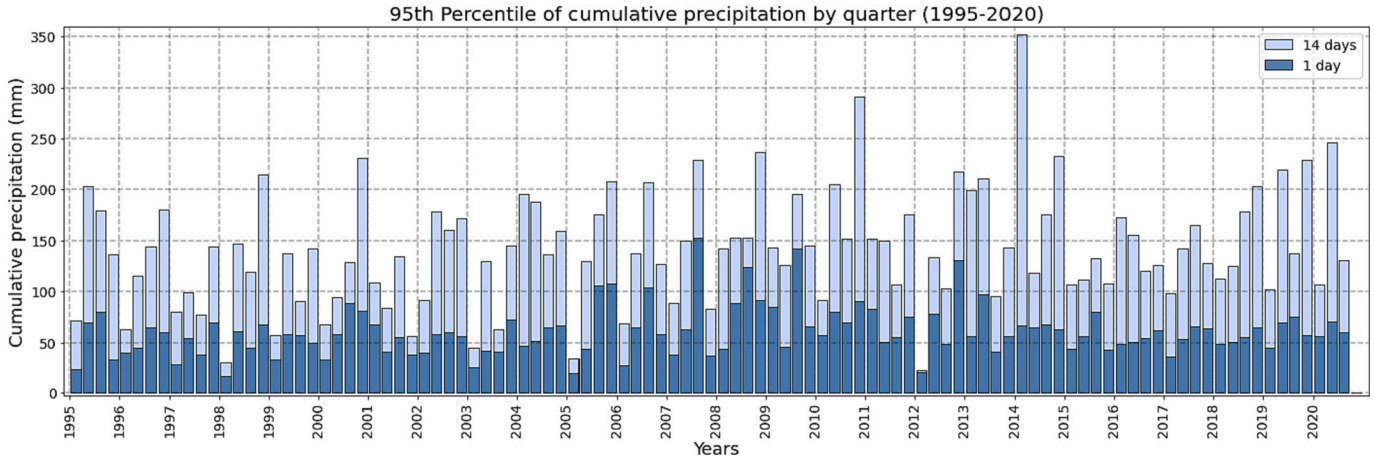

Fig. 4. The 95th percentile of cumulative precipitation for 1 and 14 consecutive days by quarter in the time period 1995–2020 in the Metropolitan City of Venice.

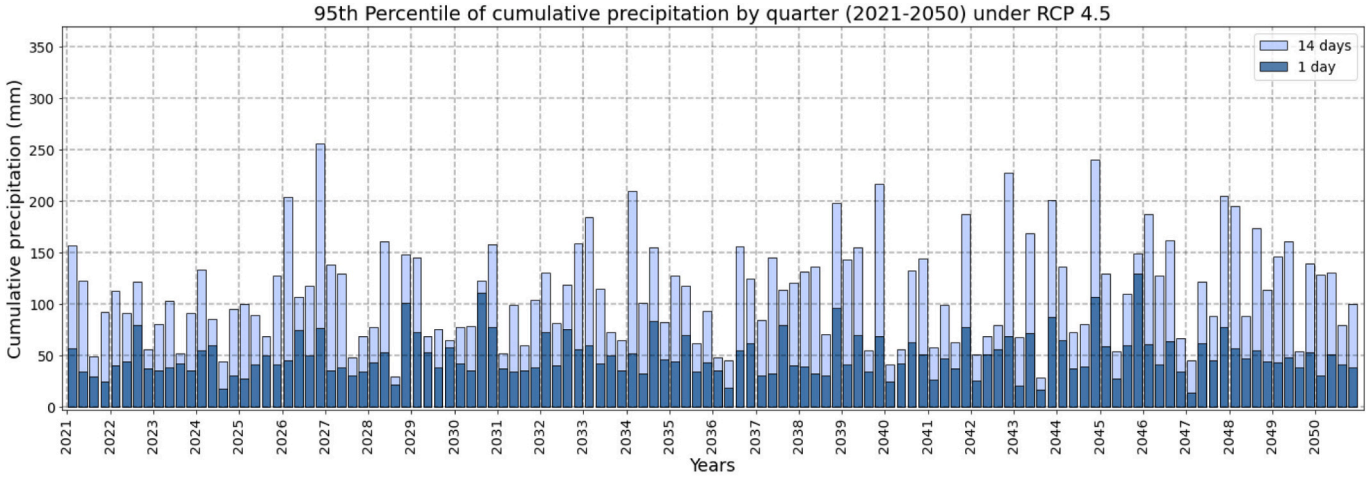

Fig. 5. The precipitation scenarios under RCP 4.5 (a) and 8.5 (b) of COSMO model for each quarter of the time period 2021–2050.

together to create a unique dataset useful to find the relations between the features and the response variable. This process is called data merging, and it consists of the integration of different datasets: triggering factors, historical pluvial flood data and precipitation. In this case study, the relation among the characteristics of the territory, precipitation (millimeters) and pluvial flood inundated areas may depend both on the spatial area and the time period in which the event occurred. The spatial domain of the case study is the Metropolitan City of Venice area, that was subdivided in 786.988 small cells with 50x50m of spatial resolution. The temporal domain regards all the quarters of 1995–2020 for the past period (i.e., 26 years, 104 quarters), and all the quarters of 2021–2050 for the future time period (i.e., 30 years, 120 quarters). It is important to mention that, for the temporal domain, triggering factors (i.e., the morphological characteristics of the territory) are assumed to remain unchanged for all the time period 1995–2050, while precipitation changes over time and pluvial flood occurrence is known for the past and it needs to be predicted for the future. Since historical pluvial flood data refers to specific single day events, they were aggregated by quarter and each of the 786.988 small areas were labelled as flooded if at least one flood event occurred in that quarter, or as non-flooded otherwise.

3.3. Machine learning models

Machine learning techniques can be applied to pluvial flood analyses to identify the most relevant patterns in the data among inundated areas, precipitation and the characteristics of the territory (i.e., the triggering factors). Pluvial flood prediction is a classification task, which aims to classify if a cell of the study area is likely to be flooded or not in a specific quarter. Four different ML models were considered in the analysis, to estimate pluvial flood risk in the most accurate way based on the 104 quarters between 1995 and 2020. The ML models taken into consideration were Logistic Regression (LR), Bayes Classifier (BC), Neural Networks (NN) and Random Forest (RF). LR, BC and RF are widely applied models for classification tasks as they are simple to implement and interpret, while NN model is more flexible to learn complex relations between the features and the response variable (Azzalini and Scarpa, 2012). Notice that NN and RF need to be trained on historical data using different configurations of their hyperparameters, i.e. parameters used to control the learning process of the model and to set their ideal model architecture (Lecun et al., 2015).

3.4. Dataset folds for spatio-temporal analysis

The assessment of pluvial flood risk is based on triggering factors, precipitation and their link with the response variable. As pluvial flood occurrence depends on the spatial characteristics of the territory and the time interval in which precipitation occurs, a specific methodology needs to be developed to consider spatio-temporal constraints. Indeed, ML models were tested to be reliable to predict pluvial flood occurrence in different spatial locations and time periods that the model has never experienced before. For this reason, the data were split in different folds, considering both time and space, in order to keep the assumption of independence between the folds in the geographical and temporal domain (Roberts et al., 2017). Hence, the dataset was split in T x S folds, where T is the number of time periods and S is the number of spatial areas in which the dataset was split up. Time intervals and spatial areas were chosen to guarantee an almost equal distribution of pluvial flood examples in each fold. Indeed, the time periods were calculated using the quantile distribution of the quarter of the flooded observation. In particular, the limits of the temporal classes are the 1/T, …, (T-1)/T quantile of the historical events with pluvial flood areas reported. The 1/T quantile divides the first and second time period, while the (T-1)/T quantile divides the second from last and the last time periods. Regarding the spatial areas, observations were grouped according to the latitude of the flooded observations to split the areas in S groups. In particular, the limits of the spatial classes were the 1/S, …, (S-1)/S quantile of the latitude of the case study area.

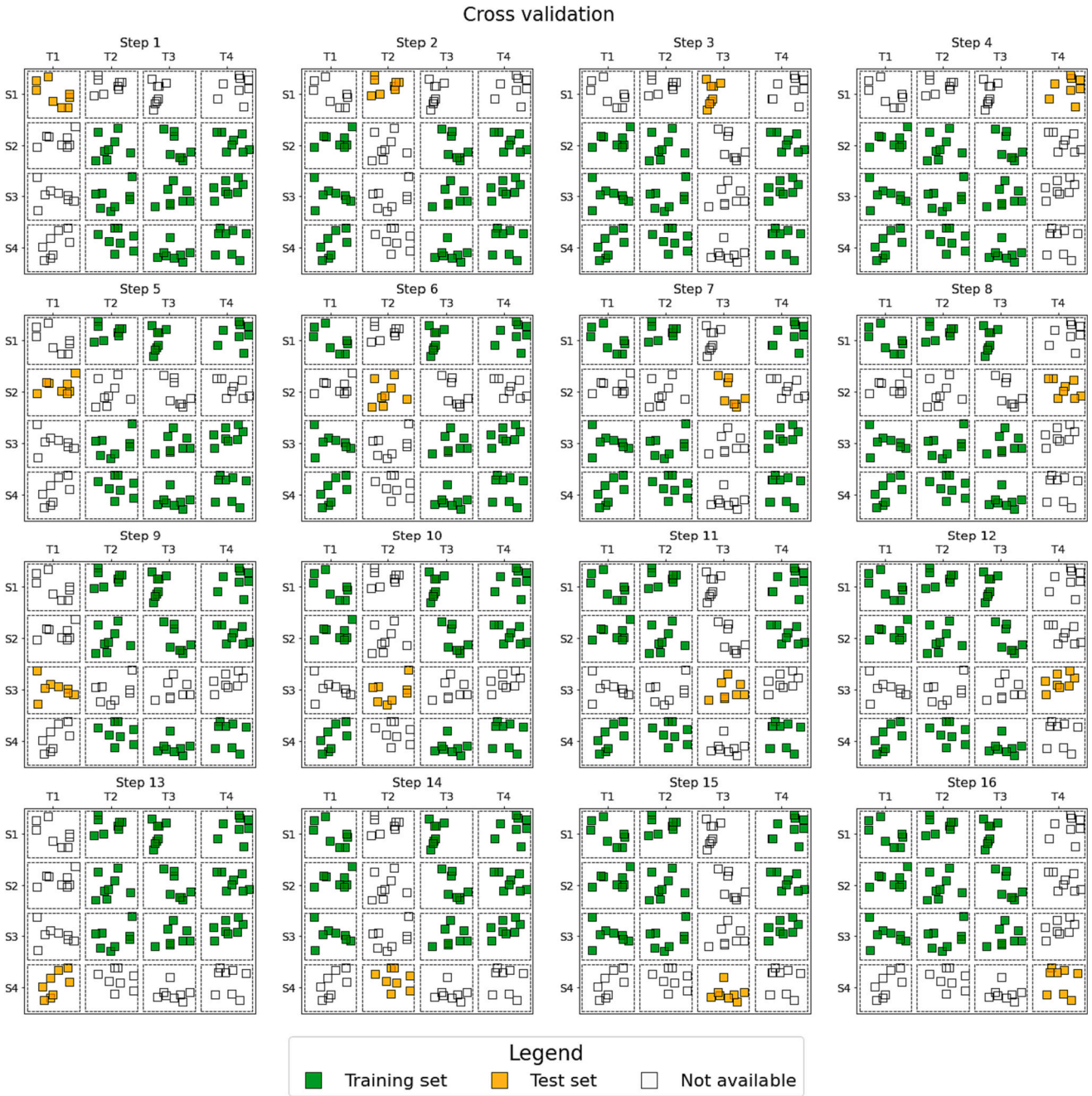

Fig. 6. The cross-validation process. At each step one of the T x S folds is the test set and (T-1) x (S-1) folds are part of the training set. In this example T = 4 and S = 4.

3.5. Cross validation for hyperparameters tuning, features selection and model selection

Usually, the performances of machine learning models to predict the response variable are assessed by splitting the dataset in two parts: the training and the test set. The training set is used by the ML models to learn the relations between the features and the response variable, while the test set measures the ability of the model to predict the response variable with data that the model has never seen before. Since the relation of pluvial flood occurrence with triggering factors and precipitation that can vary both in time and in space, we need a model able to generalize these relations for any kind of characteristics of the territory and precipitation (Meyer et al., 2018). For this reason, training and test set are not generated randomly, as it is usual in machine learning approaches, but were taken into consideration both time and space to avoid any correlation between folds. A spatio-temporal cross-validation approach was applied to get a more reliable approximation of the model accuracy to detect pluvial flood occurrence. All the possible different combination of features, hyperparameters and ML models were evaluated to obtain the best model to predict pluvial flood areas in all the T x S folds. For each combination, the evaluation of the model accuracy is composed by a series of steps. At each step, one fold $k^{t;s}$ between the T x S folds was selected to be part of the test set, (T-1) + (S-1) folds that have in common the time period or the spatial area with the test set were excluded from the analysis while the (T-1) x (S-1) independent folds were selected to be part of the training set. The procedure continues until all folds have been exactly once part of the test set, i.e., when the model has predicted all the observations of the dataset. Fig. 6 shows an example of spatio-temporal cross-validation with $T = 4$ and $S = 4$. Ideally, since the process is iterative, it is possible to evaluate the model's performances in a great number of configurations of hyperparameters and features, until it is reached the maximum value of a metric that measure the performances of the model in predicting pluvial flood in the test set. The metric adopted to evaluate ML models is the Area Under the Curve (AUC), a recommended metric used instead of the overall accuracy to compare different ML algorithms in classification problems (Bradley, 1997). As there can be a huge number of configurations based on different features and hyperparameters, the computational power may increase exponentially. For this reason, only a list of opportune hyperparameters is candidate to form the model, while a forward features selection is applied to keep only the features that are important to predict pluvial flood in the cross-validation process. As there was a relevant number of precipitation features, a constraint added on the feature selection process consists in the selection of just one precipitation feature to avoid any collinearity problem between the precipitation features, while all the triggering factors can be selected without any limit. Finally, the model that got the best AUC score in the test set during the 16 steps was selected to predict the pluvial flood inundated areas with the future scenarios of precipitation.

3.6. Pluvial flood risk mapping for past and future

3.6.1. Pluvial flood risk by quarter of the year

Once all the ML models have been trained and tested, the model that gets the best performances on the test sets based on the AUC score was selected to estimate the pluvial flood risk using its best hyperparameters and the selected features. As mentioned in Section 3.2, triggering factors are assumed to be unchanged for past and future, since no data are available for future scenarios, while precipitation data are available both for the past (from historical data of meteorological stations) and for the future (from the COSMO-CLM model). Hence, the selected model was used to estimate the risk of pluvial flood in each quarter 1995–2050, using the selected triggering factors for all the time period, historical precipitation data for 1995–2020 and the precipitation scenarios under the RCP 4.5 and 8.5 for 2021–2050. In each quarter, for each area of the case study region, the model estimated the probability of being a flooded area or not based on the features selected by the model itself.

3.6.2. Pluvial flood worst risk by quarter of the decade

In a decade time period perspective, it is possible to aggregate the information about the pluvial flood risk by quarter of the 10 years of that decade. The aggregation function used to summarize the risk of a specific decade is the calculation of the maximum risk for each cell of the study area to underline the worst risk that any area may face in 10 years. For this analysis, overall five decades have been considered, of which two for the past (2000–2009 and 2010–2019) and three for the future (2021–2030, 2031–2040 and 2041–2050).

4. Results

4.1. Dataset creation and split in spatio-temporal folds

4.1.1. Dataset

Information on the 786.988 cell areas of the case study region were collected for each quarter of the time period 1995–2020 (104 quarters) resulting in a spatio-temporal domain of 81'846'752 unique spatio-temporal observations, of which only 176'035 observations are flooded points, which is the 0.21 % of the total observations. Considering that for each unique spatio-temporal observation we need to collect 115 features (27 triggering factors and 88 precipitation indexes), the amount of data collected leads to an exponential increase of the computational costs to train the machine learning models. For this reason, a subset of 400'000 observations has been selected for further analysis: 300′000 non-flooded observations (75 %) and 100'000 flooded observations (25 %). Overall, the dataset used to train the machine learning models is composed by 400'000 unique spatio-temporal observations, 115 features and the response variable.

4.1.2. Training and test set

The objective of the proposed approach is to develop a ML model able to predict pluvial flood occurrence in different time periods and geographic locations. In ML approaches, the dataset is partitioned into training and test set. The training set is used to fit the parameters of the model, while the test set provides unbiased evaluations of the prediction errors of the model fit on the training set. The dataset was randomly split in training and test set, specifically in 16 different folds, starting from $T = 4$ temporal groups and $S = 4$ spatial groups. The 4 temporal groups of data were chosen to get an almost equal number of flooded observations in each group (in a range between 20'000 and 30'000), while the spatial groups were created using latitude as a reference in order to get an almost equal number of flooded observations in each area (about 25'000). Clearly, these thresholds guarantee an equal number of flooded observations in each spatial or temporal group, but they do not guarantee that a specific spatio-temporal fold includes any flooded observation. For example, it is possible that in a specific area, there were no flooded events in a specific temporal period. Table 2 shows the number of flood and non-flood observations for each of the 16 folds and it can be noticed that two folds do not include any flooded point.

4.2. Features and model selection

Each ML model, for a specific configuration of its hyperparameters and features, was trained and tested 16 times, until each fold was part of the test set exactly one time. As reported in Table 3, the model that obtained the best AUC score was the Logistic Regression, without any hyperparameter tuning, and the most important feature resulted to be the 14 days of cumulative precipitation (interpolated from the nearest 7 stations). Cumulative precipitation refers to the most intense 14 days of rainfall that happened in a specific quarter and indicates that flooded events are more related to consecutive days of rainfall than a single day. Since the other features only slightly improve the accuracy of the model (maximum increment of the AUC score is +0.4 %), and to be in

Table 2
The number of flood (a) and non-flood (b) observations in the dataset is grouped in 16 spatio-temporal folds.

Flood	Time				
Space	T1	T2	T3	T4	Total
S1	0	4.638	11.975	8.329	**24.942**
S2	0	6.616	8.961	9.334	**24.911**
S3	10.709	3.830	5.949	4.618	**25.106**
S4	19.510	4.872	276	383	**25.041**
Total	**30.219**	**19.956**	**27.161**	**22.664**	**100.000**

(a)

Non-flood	Time				
Space	T1	T2	T3	T4	Total
S1	15.431	7.215	2.929	5.720	**31.295**
S2	21.614	10.137	4.174	7.931	**43.856**
S3	63.172	29.808	12.430	23.700	**129.110**
S4	46.958	21.963	9.196	17.622	**95.739**
Total	**147.175**	**69.123**	**28.729**	**54.973**	**300.000**

(b)

Table 3
The AUC score in the train and test set and the selected features for each ML model.

Model	Selected features	Train AUC	Test AUC
Logistic Regression	Cumulative precipitation 14 days	0.869	**0.867**
Bayes Classifier	Cumulative precipitation 14 days	0.868	0.859
Neural Networks	Cumulative precipitation 14 days	0.851	0.830

compliance with the other models, only 14 days of cumulative precipitation was considered in the LR model, obtaining the highest AUC score between all models, hyperparameters and features tested, that is 0.867 in the test set. Therefore, the LR model with 14 days of cumulative precipitation was trained using the 400′000 observations of the dataset to better estimate the relations between the cumulative precipitation and pluvial flood risk. This final model was used to estimate pluvial flood risk in the past and to predict it in the future scenarios.

4.3. *Pluvial flood mapping*

The Logistic Regression model was run to map the risk of pluvial flood in the Metropolitan City of Venice for each quarter of the historical period 1995–2020, considering the historical precipitation data, while precipitation scenarios under RCP4.5 and 8.5 were used for the future (2021–2050). To better visualize the pluvial flood risk maps, the risk has been grouped in six classes: very low (0–20 %), low (20–40 %), medium (40–60 %), high (60–80 %), very high (80–95 %) and extremely high (95–100 %). Fig. 6 shows the percentage of the study area with pluvial flood risk above 80 % in each quarter of 1995–2020 and future quarters 2021–2050 under RCPs 4.5 and 8.5. The first bar chart of Fig. 6 shows the pluvial flood risk in each quarter of the time period 1995–2020, in which for two quarters the study area was strongly impacted (flooded areas larger than 20 %). In particular, in the 1st quarter of 2014, it was estimated that >72 % of the study area was at very high risk (80–100 %) of pluvial flood, while, in the 3rd quarter of 2006, the estimated area at medium risk was slightly >55 %. Clearly, machine learning models may overestimate the risk of pluvial flood in classification problems as the goal is to minimize both false negative (misclassified flooded areas) and false positive (misclassified unflooded areas) observations to maximize the AUC score. Indeed, in Fig. 3 the percentage of reported flooded areas in each quarter was always lower than 5 % of the total study area, while the model suggests a higher area at risk of pluvial flood in some quarters. ML estimates the probability of occurrence of the most critical events (i.e., those events in which some areas have a very high probability of pluvial flood) and not a certainty, as represented in Fig. 3 for the past monitored event. Therefore, ML models allow to identify the most vulnerable areas to pluvial flood and to capture the most critical events occurred in the past. The second bar chart of Fig. 7 represents the predicted highest risk of pluvial flood for each quarter of 2021–2050 time period, under RCP4.5. In these predictions, as in the past period, only two quarters may have a very high risk with pluvial flooded areas larger than 40 % of the study area: 4th quarter of 2026 and 4th quarter of 2044. On the other side, the third bar chart represents the predicted highest risk of pluvial flood for each quarter of 2021–2050 timeframe, under the most severe climate scenario RCP8.5, according to which 5 quarters are considered large pluvial flood events. In particular, in the 4th quarter of 2045, in the 3rd quarter of 2030 and in the 4th quarter of 2049 the predicted risk of pluvial flood covers a very relevant area: respectively the 61 %, 82 % and 71 % of the study area.

Due to the long time period from today to 2050, it is not very plausible to be certain about the exact quarter in which dangerous pluvial flood events will occur according to the precipitation scenarios. For this reason, the risks of pluvial flood were aggregated by decade, focusing on two past decades (2000–2009 and 2010–2019) and three future decades (2021–2030, 2031–2040, 2041–2050) under RCPs 4.5 and 8.5. Fig. 8 shows the highest risk classes of pluvial flood for each cell of the study area for selected past period and future decades under RCP8.5. However, further detailed maps for the whole period under study (i.e., the two past decades 2000–2009 and 2010–2019 and three future decades 2021–2030, 2031–2040 and 2041–2050) for each quarter and for the future scenarios RCP4.5 and RCP8.5 is reported in Fig. B of the Supplementary Material. The selected quarters reported in Fig. 8 show that the north-eastern side of the MCV presents extremely high risk of pluvial flood both in the past decade and in the future. This risk enlarges in the 2041–2050 period, also embracing the central part of the MCV. Overall, almost the whole study area presents very high risk of flooding events for the third quarter and under the RCP8.5.

5. Conclusions

The multiple threats posed by climate change require reliable methodologies, such as the development of ML models, to prevent disaster risk and to develop suitable response actions to increase climate resilience.

The methodology presented in this paper develops a ML model able to implement spatio-temporal constraints to improve pluvial flood risk prediction considering future scenarios of climate change, under the RCPs 4.5 and 8.5.

The produced outputs are representative of future trends of climate change and are useful for the identification of vulnerable areas to pluvial flood risk at local scale for the different scenarios. They are effective to

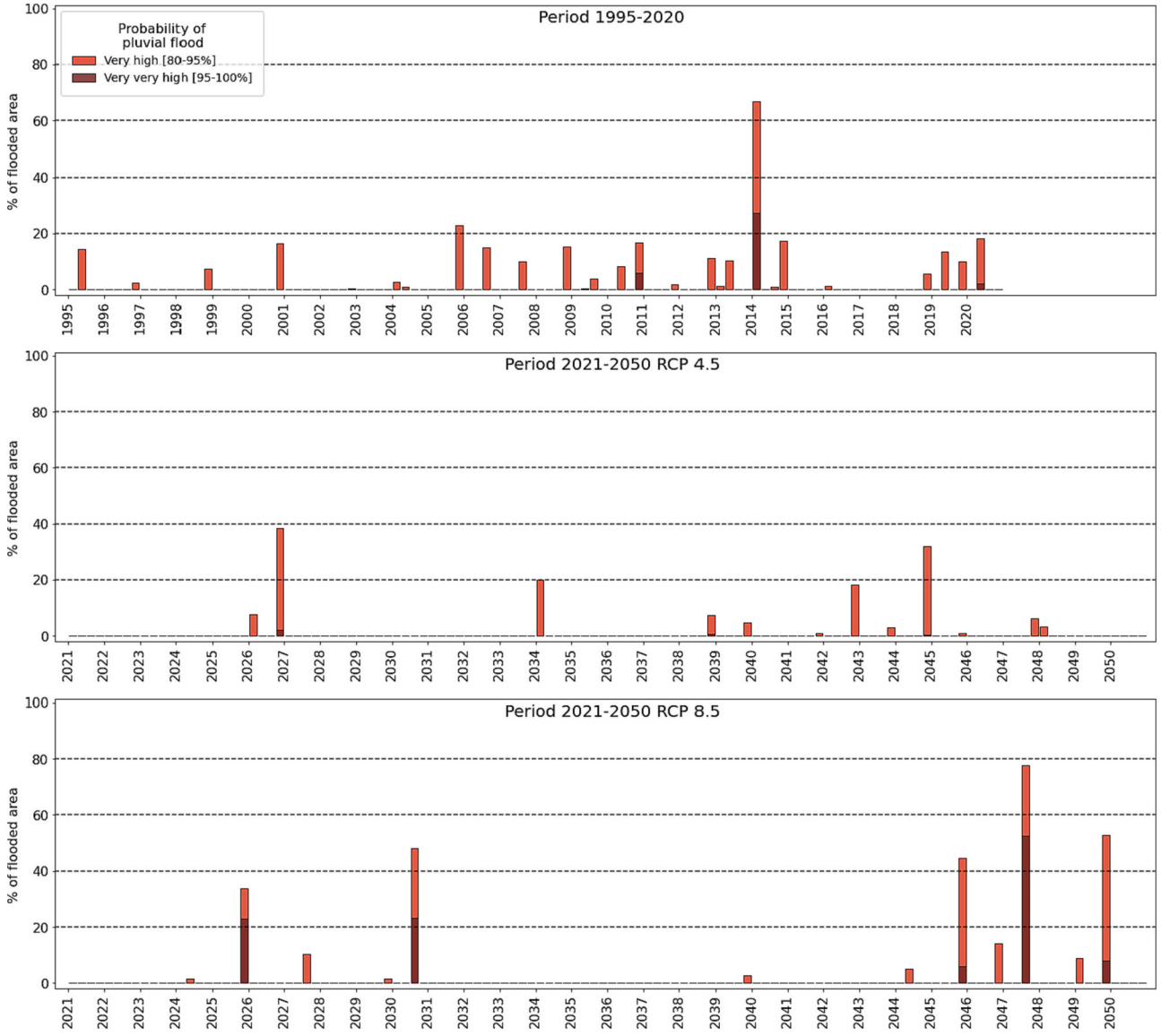

Fig. 7. The percentage of the study area at extremely high risk of pluvial flood in each quarter of 1995–2020 and future quarters 2021–2050 under RCP 4.5 and 8.5.

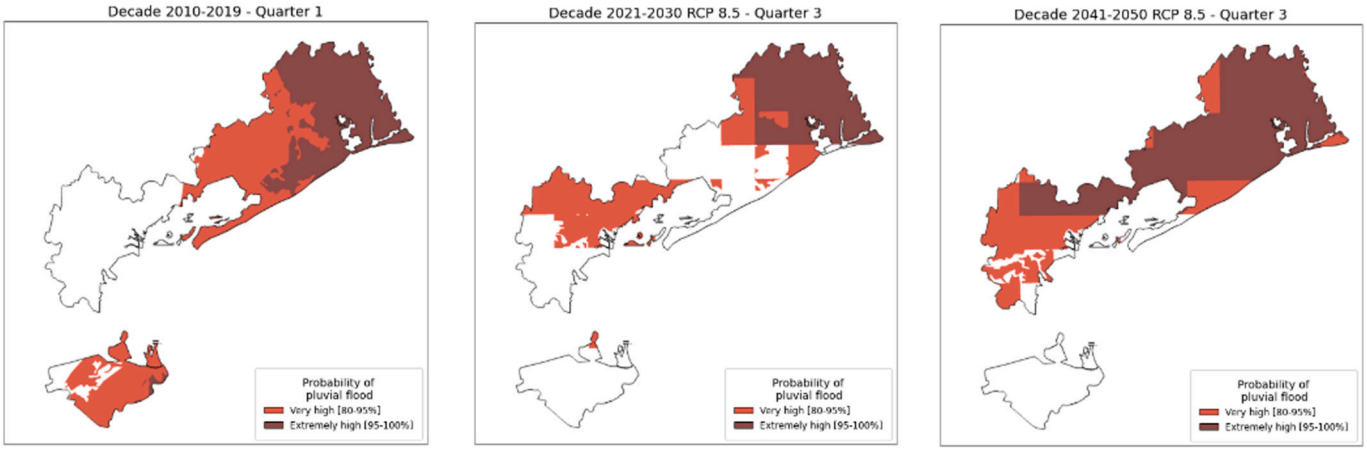

Fig. 8. The highest risks of pluvial flood for each cell of the study area for the most relevant past and future decades and quarter.

mainstream mitigative and adaptive strategies and plans (e.g., identification of hotspots and vulnerabilities, identification of mitigation and adaptation priorities as well as nature-based management solutions (e.g., O'Leary et al., 2022)) and to support decision-makers in undertaking actions and in developing early warning systems.

However, some limitations of the methodology must be acknowledged. Firstly, in the analysis only one regional climate model, COSMO-CLM, was investigated for future scenarios of precipitation, while the adoptions of multiple climate models might have made the predictions more accurate. A further limitation of the study is the 50 m spatial resolution, as a higher resolution would better support ML models and would catch stronger relationship between the territory features, the precipitation rates and the flooded areas. Future works are envisioned towards a comprehensive methodology that not only provide accurate risk flooding maps, but also rely on advanced ML techniques (e.g., Convolutional Neural Network, Graph Neural Network) for rapid prediction of flood inundation. Such methodologies are becoming largely adopted to predict, at spatio-temporal scale, water levels of flash flood events through image classification (Kabir et al., 2020; Bentivoglio et al., 2023).

CRediT authorship contribution statement

Elena Allegri: Conceptualization, Formal analysis, Investigation, Methodology, Validation, Writing – original draft. **Marco Zanetti:** Conceptualization, Data curation, Formal analysis, Methodology, Software, Writing – original draft. **Silvia Torresan:** Supervision, Writing – review & editing. **Andrea Critto:** Funding acquisition, Resources, Supervision, Writing – review & editing.

Declaration of competing interest

The authors declare that they have no known competing financial interests or personal relationships that could have appeared to influence the work reported in this paper.

Data availability

The authors do not have permission to share data.

Acknowledgements

This study is part of the Venezia2021 project, aimed at better understanding the impacts of climate change on the Metropolitan City of Venice (MCV) and its lagoon, given the environmental and cultural value of the area. The analysis performed in this work will support policy-makers and decision-makers in defining management policies to mitigate and adapt to climate change.

This research was supported by the scientific activity performed with the contribution of the Provveditorato for the Public Works of Veneto, Trentino Alto Adige and Friuli Venezia Giulia, provided through the concessionary of State Consorzio Venezia Nuova and coordinated by CORILA. The authors would also like to thank the Metropolitan City of Venice, which provided us the historical data of flooding events occurred in the case study area.

Appendix A. Supplementary data

Supplementary data to this article can be found online at https://doi.org/10.1016/j.scitotenv.2024.169925.

References

Ahiablame, L., Shakya, R., 2016. Modeling flood reduction effects of low impact development at a watershed scale. J. Environ. Manag. 171, 81–91. https://doi.org/10.1016/j.jenvman.2016.01.036.

Ahmadlou, M., et al., 2019. Flood susceptibility assessment using integration of adaptive network-based fuzzy inference system (ANFIS) and biogeography-based optimization (BBO) and BAT algorithms (BA). Geocarto Int. 34 (11), 1252–1272. https://doi.org/10.1080/10106049.2018.1474276.

Apel, H., et al., 2016. Combined fluvial and pluvial urban flood hazard analysis: \hack{\newline} concept development and application to Can Tho city, \hack{\newline} Mekong Delta, Vietnam. Nat. Hazards Earth Syst. Sci. 16 (4), 941–961. https://doi.org/10.5194/nhess-16-941-2016.

Arabameri, A., et al., 2019. A comparison of statistical methods and multi-criteria decision making to map flood hazard susceptibility in Northern Iran. Sci. Total Environ. 660, 443–458. https://doi.org/10.1016/j.scitotenv.2019.01.021.

ARPAV, 2007. In: Barbi, A., Formentini, G., Monai, M., Rech, F., Zardini, F. (Eds.), Analisi meteo-climatica dell'evento pluviometrico del 26 settembre 2007 nel veneziano. Available at: http://www.ingmaurogallo.com/documenti/Analisi%20ARPAV%20MeteoClimatica%20evento%2026.09.07.pdf.

Asadieh, B., Krakauer, N.Y., 2017. Global change in streamflow extremes under climate change over the 21st century. Hydrol. Earth Syst. Sci. 21 (11), 5863–5874. https://doi.org/10.5194/hess-21-5863-2017.

Aslan, S., et al., 2022. Recurrent neural networks for water quality assessment in complex coastal lagoon environments: a case study on the Venice Lagoon. Environ. Model. Softw. 154 (2022), 105403.

Azzalini, A., Scarpa, B., 2012. Data Analysis and Data Mining: An Introduction. OUP USA.

Bentivoglio, R., et al., 2023. Rapid Spatio-temporal flood modelling via hydraulics-based graph neural networks. EGUsphere 2023, 1–24. https://doi.org/10.5194/egusphere-2023-284.

Blanc, J., Hall, J., Roche, N., Dawson, R., Cesses, Y., Burton, A., Kilsby, C., 2012. Enhanced efficiency of pluvial flood risk estimation in urban areas using spatial-temporal rainfall simulations. J. Flood Risk. Manag. 5 (2), 143–152.

Bradley, A.P., 1997. The use of the Area under the ROC Curve in the evaluation of Machine Learning algorithms. Patt. Recognit. 30 (7), 1145–1159.

Chowdary, M., et al., 2013. Multi-criteria decision making approach for watershed prioritization using analytic hierarchy process technique and GIS. Water Resour. Manag. 27 https://doi.org/10.1007/s11269-013-0364-6.

Chowdhuri, I., Pal, S.C., Chakrabortty, R., 2020. Flood susceptibility mapping by ensemble evidential belief function and binomial logistic regression model on river basin of eastern India. Adv. Space Res. 65 (5), 1466–1489. https://doi.org/10.1016/j.asr.2019.12.003.

Deng, W., et al., 2013. Flood disaster evaluation model based on kernel dual optimization support vector machine. Inf. Technol. J. 12, 2412–2418. https://doi.org/10.3923/itj.2013.2412.2418.

Dipartimento per gli Affari Regionali e le Autonomie, 2017. I dossier della Città Metropolitana di Venezia. Città Metropolitana di Venezia.

Ebers, N., Schroter, K., Muller-Thomy, H., 2023. Estimation of future rainfall extreme values by temperature-dependent disaggregation of climate model data. EGUsphere. https://doi.org/10.5194/egusphere-2023-1948.

Guo, Z., et al., 2021. Data-driven flood emulation: speeding up urban flood predictions by deep convolutional neural networks. J. Flood Risk Manag. 14 (1), 1–14. https://doi.org/10.1111/jfr3.12684.

Herath, H.M.M., Wijesekera, N.T.S., 2019. A state-of-the-art review of flood risk assessment in urban area. IOP Conf. Ser. Earth Environ. Sci. 281 (1), 12029. https://doi.org/10.1088/1755-1315/281/1/012029.

IPCC, 2021. Climate change 2021 the physical science basis WGI. Bull. Chin. Acad. Sci. 34 (2), F0003.

ISTAT, 2022. http://dati.istat.it/Index.aspx?DataSetCode=DCIS_POPRES1.

Jiang, R., Lu, H., Yang, K., Chen, D., Zhou, J., Yamazaki, D., Pan, M., Li, W., Xu, N., Yang, Y., Guan, D., Tian, F., 2023. Substantial increase in future fluvial flood risk projected in China's major urban agglomerations. Commun. Earth Environ. 4, 389.

Kabir, S., et al., 2020. A deep convolutional neural network model for rapid prediction of fluvial flood inundation. J. Hydrol. 590, 125481 https://doi.org/10.1016/j.jhydrol.2020.125481.

Khosravi, K., et al., 2019. A comparative assessment of flood susceptibility modeling using multi-criteria decision-making analysis and machine learning methods. J. Hydrol. 573, 311–323. https://doi.org/10.1016/j.jhydrol.2019.03.073.

Kia, M.B., et al., 2012. An artificial neural network model for flood simulation using GIS: Johor River Basin, Malaysia. Environ. Earth Sci. 67 (1), 251–264.

Kundzewicz, Z.W., Pińskwar, I., Brakenridge, G.R., 2013. Large floods in Europe, 1985–2009. Hydrol. Sci. J. 58 (1), 1–7. https://doi.org/10.1080/02626667.2012.745082.

Lecun, Y., Bengio, Y., Hinton, G., 2015. Deep learning. Nature 521 (7553), 436–444. https://doi.org/10.1038/nature14539.

Lee, M.-J., Kang, J., Jeon, S., 2012. Application of frequency ratio model and validation for predictive flooded area susceptibility mapping using GIS. In: 2012 IEEE International Geoscience and Remote Sensing Symposium, pp. 895–898. https://doi.org/10.1109/IGARSS.2012.6351414.

Merz, B., Kreibich, H., Lall, U., 2013. Multi-variate flood damage assessment: a tree-based data-mining approach. Nat. Hazards Earth Syst. Sci. 13 (1), 53–64. https://doi.org/10.5194/nhess-13-53-2013.

Meyer, H., et al., 2018. Improving performance of spatio-temporal machine learning models using forward feature selection and target-oriented validation. Environ. Model. Softw. 101, 1–9. https://doi.org/10.1016/j.envsoft.2017.12.001.

Miller, J.D., Hutchins, M., 2017. The impacts of urbanisation and climate change on urban flooding and urban water quality: a review of the evidence concerning the United Kingdom. J. Hydrol. Region. Stud. 12 (June), 345–362. https://doi.org/10.1016/j.ejrh.2017.06.006.

Nowakowska, M., et al., 2017. 'Identifi cation, Calibration and Validation of Hydrodynamic Model of Urban Drainage System in the example of the City of Wroclaw', Ochrona Środowiska, 39, pp. 51–60.
O'Leary, B., et al., 2022. Embracing nature-based solutions to promote resilient marine and coastal ecosystems. Nat.-Based Solut. 3, 100044.
Peleg, N., Ban, N., Gibson, M.J., Chen, A.S., Paschalis, A., Burlando, P., Leitao, J.P., 2022. Mapping storm spatial profiles for flood impact assessments. Adv. Water Resour. 166, 104258.
Pham, B.T., et al., 2020. A comparative study of kernel logistic regression, radial basis function classifier, multinomial Naïve Bayes, and logistic model tree for flash flood susceptibility mapping. Water 12 (1). https://doi.org/10.3390/w12010239.
Pradhan, B., 2009. Flood susceptible mapping and risk area delineation using logistic regression, GIS and remote sensing. J. Spat. Hydrol. 9 (2), 1–18.
Rahmati, O., Pourghasemi, H.R., Zeinivand, H., 2016. Flood susceptibility mapping using frequency ratio and weights-of-evidence models in the Golastan Province, Iran. Geocarto Int. 31 (1), 42–70. https://doi.org/10.1080/10106049.2015.1041559.
Roberts, D.R., et al., 2017. Cross-validation strategies for data with temporal, spatial, hierarchical, or phylogenetic structure. Ecography 40 (8), 913–929. https://doi.org/10.1111/ecog.02881.
Roy, P., et al., 2020. Threats of climate and land use change on future flood susceptibility. J. Clean. Prod. 272, 122757 https://doi.org/10.1016/j.jclepro.2020.122757.
Shahabi, H., et al., 2021. Flash flood susceptibility mapping using a novel deep learning model based on deep belief network, back propagation and genetic algorithm. Geosci. Front. 12 (3), 101100. https://doi.org/10.1016/j.gsf.2020.10.007.
Spano, D., et al., 2020. Analisi del rischio. I cambiamenti climatici in Italia.
Sperotto, A., et al., 2015. A multi-disciplinary approach to evaluate pluvial floods risk under changing climate: the case study of the municipality of Venice (Italy). Sci. Total Environ. 562, 1031–1043. https://doi.org/10.1016/j.scitotenv.2016.03.150.
Szewrański, S., et al., 2018. Pluvial Flood Risk Assessment tool (PFRA) for rainwater management and adaptation to climate change in newly urbanised areas. Water 10 (4). https://doi.org/10.3390/w10040386.
Tehrany, M.S., Pradhan, B., Jebur, M.N., 2013. Spatial prediction of flood susceptible areas using rule based decisiontree (DT) and a novel ensemble bivariate and multivariate statisticalmodels in GIS. J. Hydrol. 504, 69–79.
Tehrany, M.S., Pradhan, B., Jebur, M.N., 2014. Flood susceptibility mapping using a novel ensemble weights-of-evidence and support vector machine models in GIS. J. Hydrol. 512, 332–343.
Tingsanchali, T., Karim, F., 2010. Flood-hazard assessment and risk-based zoning of a tropical flood plain: case study of the Yom River, Thailand. Hydrol. Sci. J. 55 (2), 145–161. https://doi.org/10.1080/02626660903545987.
UNESCO, 2020. Water and climate change. Int. Encycl. Geogr. https://doi.org/10.1002/9781118786352.wbieg0793.pub2.
UNISDR, & C. for R. on the E. of D, 2015. The Human Cost of Weather Related Disasters 1995–2015. Institute of Health and Society Université Catholique de Louvain (UCL), Belgium, Centre for Research on the Epidemiology of Disasters, p. 2015. Available at: http://weekly.cnbnews.com/news/article.html?no=124000.
Venice Province, 2011. In: Vitturi, A. (Ed.), Atlante geologico della Provincia di Venezia. Cartografie e note illustrative, Provincia di Venezia.
Wagenaar, D., et al., 2020. Invited perspectives: how machine learning will change flood risk and impact assessment. Nat. Hazards Earth Syst. Sci. 20 (4), 1149–1161. https://doi.org/10.5194/nhess-20-1149-2020.
Wang, Y., et al., 2020. Flood susceptibility mapping using convolutional neural network frameworks. J. Hydrol. 582 (December 2019), 124482. https://doi.org/10.1016/j.jhydrol.2019.124482.
Wheater, H.S., 2006. Flood hazard and management: a UK perspective. Philos. Trans. R. Soc. A Math. Phys. Eng. Sci. 364 (1845), 2135–2145. https://doi.org/10.1098/rsta.2006.1817.
Zanetti, M., Allegri, E., Sperotto, A., Torresan, S., Critto, A., 2022. Spatio-temporal cross-validation to predict pluvial flood events in the Metropolitan City of Venice. J. Hydrol. 612 (PB), 128150. https://doi.org/10.1016/j.jhydrol.2022.128150.
Zennaro, F., et al., 2021. Exploring machine learning potential for climate change risk assessment. Earth Sci. Rev. 220 (February), 103752. https://doi.org/10.1016/j.earscirev.2021.103752.